CONFINED FLUID ^{3}He: THERMODYNAMIC PROPERTIES AND CRITICAL BEHAVIOR IN QUASI-ONE DIMENSION

G. H. BORDBAR[1,2,3], M. A. RASTKHADIV[1]

[1]Department of Physics, Shiraz University, Shiraz 71454, Iran*
[2]Department of Physics and Astronomy, University of Waterloo, 200 University Avenue West, Waterloo, Ontario N2L3G1, Canada
[3]Perimeter Institute for Theoretical Physics, 31 Caroline Street North, Waterloo, Ontario, N2L 2Y5, Canada
E-mail: ghbordbar@shirazu.ac.ir

Received December 15, 2017

Abstract. A variational approach has been used to study the behavior of fluid ^{3}He confined in a single-wall carbon nanotube at finite temperature $(1-4$ K$)$. We have calculated the energy of system by employing the variational method based on the quantum cluster expansion of the energy. Then, some thermodynamic properties such as entropy, free energy, equation of state, compressibility and specific heat have been investigated. This study has been done for a density range of $0.1-1.0$ nm^{-1} and three different carbon nanotube radii, $R=0.3, 0.48$ and 0.8 nm. Our result for the equation of state shows a liquid-gas second order phase transition for this confined system at a density and temperature which depend on the nano-tube radius. The critical behavior of this system has been studied, and the relevant critical exponents have been verified by Griffiths inequality. The remarkable point of this study is the low density and pressure of transition point in comparison with no confined case. This phenomenon is differentiated from the strong adsorption of ^{3}He atoms by the carbon nanotube wall.

Key words: Confined system, fluid ^{3}He, thermodynamic properties, carbon nanotube, quasi-one-dimensional, second order phase transition.

PACS: 67.30.ef, 68.35.Gy.

1. INTRODUCTION

Cold fermionic gases were observed for the first time in 1999 by Marco *et al.* [1]. After this exploration, scientists detected anomalous behavior in these degenerate Fermi systems. For instance, superfluidity of a Fermi gas was obtained in 2003 [2] which allowed for the exploration of Bose Einstein condensation in fermionic systems. These interesting properties has led to a numerous works on ultra-cold polarized and normal fermionic gases [3–7]. Helium as an inert gas is a prominent system in this category since it remains as a gas until near absolute zero. Fluid helium behaves in a different manner in the low dimensions in contrast with that of bulk case. For example in recent years the properties of helium in two dimensions

*Permanent address

were investigated by some theoretical and experimental scientists [8–17], while in present work our focus is on quasi-one dimensional behavior of fluid ^{3}He. One of the practical methods to verify a fluid in quasi-one-dimension (Q1D) is using carbon nanotubes [18], although to have a quantum fluid, the temperature should be low enough to freeze out the azimuthal motion. It is worth to noting that the atomic structure of single-wall carbon nanotubes (SWCN) is characterized by a chiral index (n, m) [19]. For example $(7, 7)$ nanotube means a SWCN with radius $R = 0.4813$ nm. There is no binding between ^{3}He atoms for one dimension $(1D)$ and three dimensions $(3D)$, because of their small mass and fermionic characteristic, although in Q1D according to radius of the tube, it is possible [9]. Many works have been done in this area which can be divided into two groups: 1) calculation of the binding energy of a few ^{3}He atoms in a SWCN [9–11], 2) verification of thermodynamic behavior of fluid ^{3}He in a SWCN [8, 12, 13]. The realistic collective behavior of fluid ^{3}He in a SWCN may not be properly comprehended by both groups. The reason is that the first group has considered only few particles, and the second has ignored ^{3}He-^{3}He [8] or ^{3}He-C interactions [12, 13].

In recent years, we have studied the properties of normal and polarized fluid ^{3}He at zero and finite temperatures, in quasi-one, two and three dimensions [20–29]. Very recently, we have investigated the ground state thermodynamic properties of fluid ^{3}He injected in a SWCN [17]. The main aim of that work was to investigate the collective behavior of ^{3}He atoms in an attractive space of carbon nanotube. This goal will be satisfied by a complicated many-body calculations which is almost impossible by some techniques such as the Monte Carlo methods (since the number of particles is very large). In the present paper, we intend to calculate the thermodynamic properties of fluid ^{3}He injected in a carbon nanotube at finite temperature by a variational method based on quantum cluster expansion of energy [30–32]. We consider both ^{3}He-^{3}He and ^{3}He-C interactions by Lennard-Jones potential (V_{LJ}) [33] and Stan-Cole potential (V_{SC}) [34] respectively. The Stan-Cole potential is the mean field of whole carbon atoms which can be felt by a single ^{3}He atom. By considering ^{3}He-C interaction, the thermodynamic behavior of fluid ^{3}He will change very much [17]. Calculations will be done for ^{3}He density range $0.1 - 1.0$ nm^{-1} and three different carbon nanotubes with radii $R = 0.3,\ 0.48$ and 0.8 nm for four specific temperatures $T = 1,\ 2,\ 3$ and 4 K.

2. METHOD

In this section a useful many-body approach is introduced to determine the collective behavior of fluid ^{3}He injected in a SWCN. This variational method which is based on quantum cluster expansion of energy, enables us to calculate the total energy and total wave function of this interacting system [35].

2.1. LOWEST ORDER VARIATIONAL FORMALISM

In the lowest order variational method, the total wave function of the system is defined as the product of single particle wave functions and a many-body correlation function,

$$\psi(1,2,...,N) = F(1,2,...,N)\phi(1,2,...,N), \tag{1}$$

where ϕ is the total wave function of non-interacting particles (Slater determinant for fermionic systems) and F is the N-body correlation function. We consider the correlation function in a Jastrow form,

$$F(1,2,...,N) = \prod_{i>j} f(ij), \tag{2}$$

where $f(ij)$ is the two-body correlation function. Based on the quantum cluster expansion, the total energy can be written as follows [35],

$$E = \frac{\langle \Psi | \, H \, | \Psi \rangle}{\langle \Psi \mid \Psi \rangle} = E_1 + E_2 + ..., \tag{3}$$

where E_1 is the one-body cluster energy, E_2, the two-body cluster energy, and etc. As the range of interaction potential becomes shorter, the higher order terms of the energy cluster expansion will have less contributions [36].

At finite temperature, the one-body energy (E_1) is given by the following relation,

$$E_1 = \sum_k n(k)\varepsilon(k), \tag{4}$$

where

$$n(k) = \frac{1}{e^{\beta(\varepsilon(k)-\mu)}+1}, \tag{5}$$

is the Fermi-Dirac distribution function. In the above equation $\varepsilon(k)$ is the single particle energy, $\beta = \frac{1}{k_B T}$ and μ is the chemical potential. For each density and temperature, the chemical potential can be obtained by the following constraint,

$$N = \sum_k \frac{1}{e^{\beta(\varepsilon(k)-\mu)}+1}. \tag{6}$$

At finite temperature, the two-body energy has the following form,

$$E_2 = \frac{1}{2}\sum_{i,j} n(k_i)n(k_j)\langle ij|\omega(12)\,|ij-ji\rangle, \tag{7}$$

where $\omega(12)$ is the two-body effective potential,

$$\omega(12) = \frac{\hbar^2}{m}[\bigtriangledown f(r)]^2 + f^2(r)V(r). \tag{8}$$

In above equation, $V(r)$ is the inter-particle potential and $f(r)$ is the two-body correlation function.

2.2. LOWEST ORDER VARIATIONAL CALCULATIONS FOR FLUID ^{3}He INJECTED IN A SWCN AT FINITE TEMPERATURE

Our system is a SWCN with radius R and length L containing ^{3}He atoms which feel both ^{3}He-^{3}He and ^{3}He-C interactions. We consider the Lennard-Jones potential (V_{LJ}) for ^{3}He-^{3}He interaction (inter-particle potential), and Stan-Cole potential (V_{SC}) for ^{3}He-C interaction,

$$V_{LJ}(r) = 4\epsilon_1 \left[\left(\frac{\lambda}{\rho}\right)^{12} - \left(\frac{\lambda}{\rho}\right)^{6} \right], \tag{9}$$

$$V_{SC}(\rho : R) = 3\pi\theta\epsilon_2\sigma^2 \left[\frac{21}{32} \left(\frac{\sigma}{R}\right)^{10} M_{11}(x) - \left(\frac{\sigma}{R}\right)^{4} M_5(x) \right], \tag{10}$$

$$M_m(x) = \int_0^{\pi} d\varphi \frac{1}{(1+x^2-2x\cos\varphi)^{\frac{m}{2}}}, \tag{11}$$

where R is the radius of nanotube, ρ is the distance from the axis of nanotube, $x = \frac{\rho}{R}$, $\epsilon_1 = 10.22$ K, $\lambda = 0.2556$ nm, $\epsilon_2 = 3.18$ K, $\sigma = 0.274$ nm and $\theta = 38$ nm^{-2} is the surface density of carbon atoms of nanotube. Now, we employ the following two-body correlation function for ^{3}He atoms,

$$f(r,n,T) = 1 - e^{-\zeta r^2}, \tag{12}$$

where $\zeta = \zeta(n,T)$ is a density and temperature dependent variational parameter. We choose this form for correlation function because as r goes to zero, the correlation function should approach to zero, and as r goes to infinity, the correlation function should approach to unity. For each value of density and temperature, we minimize the two-body energy with respect to the variation in parameter ζ. This minimization enables us to gain a realistic correlation function.

To compute E_1 and E_2 for fluid ^{3}He injected in a carbon nanotube, we need to have single particle energy ($\varepsilon(k)$) and single particle wave function (ϕ). To find $\varepsilon(k)$, we should solve the problem of a particle (^{3}He) in a cylindrical box which is under an external potential effect caused by carbon atoms of nanotube (V_{SC}). So, we apply the following Schrödinger equation,

$$-\frac{\hbar^2 \bigtriangledown^2}{2m^*}\phi + V_{SC}\phi = \varepsilon\phi. \tag{13}$$

Here, m^* is effective mass which is considered as a variational parameter in our calculations. Since our container is a carbon nanotube, it is more convenient to use

cylindrical coordinates (ρ, φ, z). Thus Eq. (13) can be rewritten as follows,

$$\begin{aligned} &\frac{1}{\rho}\frac{\partial}{\partial\rho}\left(\rho\frac{\partial\phi}{\partial\varphi}\right)+\frac{1}{\rho^2}\frac{\partial^2\phi}{\partial\varphi}+\frac{\partial^2\phi}{\partial z^2} \\ &+\left[\eta_1 M_{11}(x)+\eta_2 M_5(x)\right]\phi+\eta_3\varepsilon\phi=0, \end{aligned} \tag{14}$$

where $\eta_1 = -4.28\times10^{-3}$, $\eta_2 = 4.483\times10^{-1}$ and $\eta_3 = 1.08\times10^{-1}$. According to the fact that V_{SC} does not depend on z coordinate, we can separate Eq. (14) into two parts by considering the following wave function,

$$\phi(\rho,\varphi,z)=\phi_1(\rho,\varphi)\phi_2(z), \tag{15}$$

where $\phi_1(\rho,\varphi)$ is related to coordinates ρ and φ, and $\phi_2(z)$ is related to coordinate z. By inserting Eq.(15) into Eq.(14) and using separation of variables, the differential equation is converted to two parts,

$$\begin{aligned} &\frac{1}{\rho}\frac{\partial}{\partial\rho}\left(\rho\frac{\partial\phi_1(\rho,\varphi)}{\partial\varphi}\right)+\frac{1}{\rho^2}\frac{\partial^2\phi_1(\rho,\varphi)}{\partial\varphi} \\ &+\left[\eta_1 M_{11}(x)+\eta_2 M_5(x)\right]\phi_1(\rho,\varphi) \\ &+\eta_3\varepsilon(k_{\rho,\varphi})\phi_1(\rho,\varphi)=0, \end{aligned} \tag{16}$$

$$\frac{\partial^2\phi_2(z)}{\partial z^2}+\eta_3\varepsilon(k_z)\phi_2(z)=0, \tag{17}$$

where $\varepsilon(k_{\rho,\varphi})$ and $\varepsilon(k_z)$ are the single particle energy related to coordinates (ρ,φ) and z, respectively. The first equation should be solved numerically, whereas the second equation has an analytic solution $\phi(z) = sin(k_z z)$. By inserting the boundary conditions, the single particle energy $\varepsilon(k) = \varepsilon(k_z) + \varepsilon(k_{\rho,\varphi})$ will have the discrete values corresponding to the quantum numbers n_ρ, n_φ and n_z.

To compute the one-body energy, we can insert $\varepsilon(k)$ into Eq. (4) and change the summation to an integral by considering the density of states,

$$\frac{E_1}{N}=\frac{1}{\pi n}\int_0^\infty n(k_z)\varepsilon(k_z)dk_z+\sum_{k_{\rho,\varphi}} n(k_{\rho,\varphi})\varepsilon(k_{\rho,\varphi}), \tag{18}$$

where $\frac{E_1}{N}$ is the one-body energy per particle, and $\mathfrak{n} = \frac{N}{L}$ is number density.

Now for calculating the two-body energy of ^{3}He atoms, we insert the inter-particle potential $V_{LJ}(r)$ and the two-body correlation function in Eq. (8) to get the effective potential. Finally, using the computed single particle wave function and the

effective potential, the two-body energy (Eq. (7)) gets the follow form,

$$E_2 = A\int\int d^3r_1 d^3r_2 \phi^2(\rho_1,\varphi_1)\phi^2(\rho_2,\varphi_2)\omega(12) \times \sum_{k_i k_j} n(k_i)n(k_j)\sin(k_i z_1)\sin(k_j z_2) \times \left[\sin(k_i z_1)\sin(k_j z_2) - \tfrac{1}{2}\sin(k_j z_1)\sin(k_i z_2)\right], \quad (19)$$

where A is the normalization coefficient. As we mentioned in the previous section, $\zeta = \zeta(n,T)$ is a density and temperature dependent variational parameter, so we minimize E_2 with respect to ζ for each value of density and temperature.

Finally, the thermodynamic properties of system can be obtained from the free energy, $F = E - TS$, where

$$S = -k_B \sum_k \left[(1-n(k))\ln(1-n(k)) + n(k)\ln(n(k))\right], \quad (20)$$

is the entropy of system. As it was mentioned previously, we consider the effective mass as a variational parameter. In fact, we minimize the free energy of system with respect to the variation of effective mass. This procedure is done numerically.

3. RESULTS AND DISCUSSIONS

As it was mentioned before, in our previous work, we have already investigated the thermodynamic properties of a quasi-one dimensional fluid ^{3}He at finite temperature without considering the effect of interaction with the container [6]. In that work, no phase transition was seen. Whereas in present work, the interaction with the container has been considered for ^{3}He-C. Our calculations show that by inserting this interaction, the one-body energy decreases extremely to the negative values which indicates that ^{3}He-C interaction is very strong. Although the main purpose of this work is to determine the collective behavior of ^{3}He particles in a SWCN, we prefer to compare our findings for the single particle energy with the other results. Thus, we have used three specific radii $R = 0.3$, 0.48 and 0.8 nm for our system. Vranjes *et al.* [2] have calculated single particle binding energy of one ^{3}He atom in a SWCN for mentioned radii. Our results for single particle energy at the ground state ($n_\rho = 1$ and $n_\varphi = 0$) with $R = 0.3$, 0.48 and 0.8 nm are $\varepsilon = -427.21$, -231.671 and -161.521 K, respectively. The mentioned authors results are $\varepsilon = -423.813$,-231.665 and -159.716 K for $R = 0.34$, 0.48 and 0.82 nm, respectively. As we see, there is a good agreement between both works.

Now we are going to verify the thermodynamic behavior of the system, thus the total energy is required (Eq. (3)). The first term of total energy is the one-body energy which has been shown in Fig. 1 for $R = 0.48$ nm where ε_0 is the ground state energy. In fact E_1 is differentiated from the kinetic energy and ^{3}He-C interaction energy.

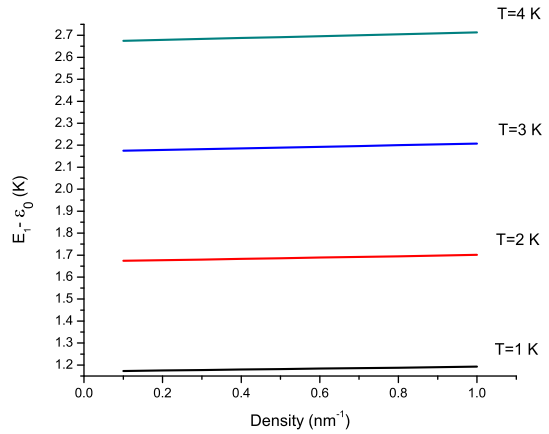

Fig. 1 – One-body energy per particle *versus* density for $R = 0.48$ nm at different temperatures (T). Here $\varepsilon_0 = -231.671$ K.

In present work the magnitude of E_1 decreases extremely to the negative values, however in our previous work E_1 was positive for all densities. This indicates a high attraction of ^{3}He atoms by SWCN. E_1 increases by increasing both temperature and density although this is more obvious for temperature. The second term of energy cluster expansion (E_2) has been presented in Fig. 2 for $R = 0.48$ nm which indicates the ^{3}He-^{3}He interaction energy. E_2 increases by rising density, although it decreases by increasing the temperature. As it is shown, E_2 decreases compared to the case in which the interaction with the wall has been ignored [6], due to the fact that in present work the two body wave function has been modified by ^{3}He-C interaction. As we discussed before in the cluster expansion method, if the inter-atomic potential is short range, the higher order of energy expansion terms can be ignored. According to the fact that the inter-atomic potential of our system is Lennard-Jones type, we can easily ignore the higher order terms. Now by adding E_1 and E_2, the total energy of the system is obtained. We have found that the total energy has large negative values, which shows that ^{3}He atoms form an strong bounded fluid in SWCN where a liquid-gas phase transition may not be unexpected.

The entropy of the system have been calculated by applying Eq. (20), which has been plotted in Fig. 3. As we expected the entropy increases by increasing the temperature, while it decreases by rising the density. Since in a fixed temperature there exist definite accessible energy states, therefore by increasing the density the number of unoccupied states reduces leading to reduction of entropy. Whereas by rising temperature the number of these accessible states will increase. Now, using the total energy and entropy, we can compute the free energy to find out the thermo-

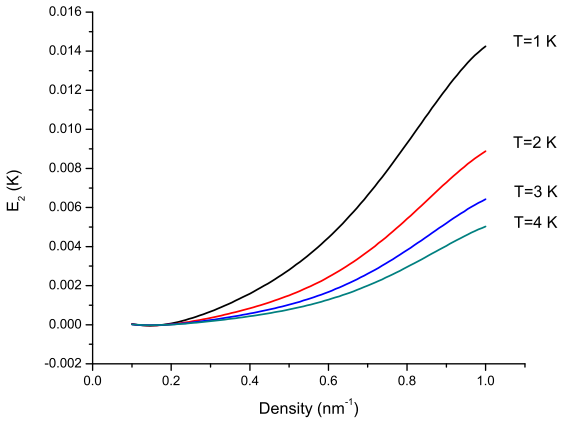

Fig. 2 – Two-body energy per particle *versus* density for radius $R = 0.48$ nm at different temperatures (T).

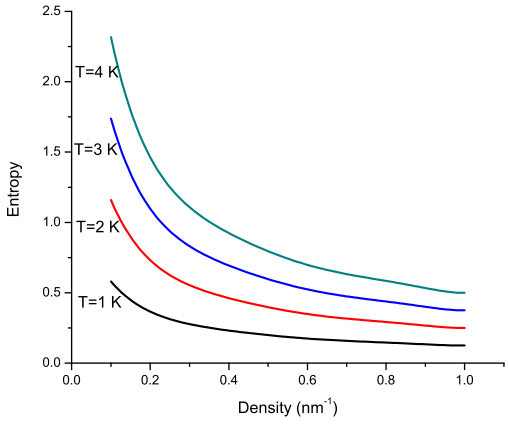

Fig. 3 – Entropy per particle *versus* density for radius $R = 0.48$ nm at different temperatures (T).

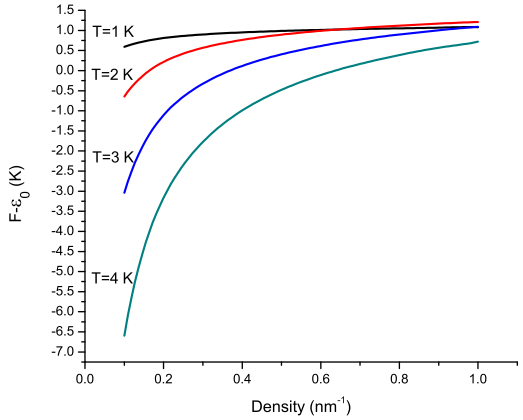

Fig. 4 – Free energy per particle *versus* density for $R = 0.48$ nm at different temperatures (T). Here $\varepsilon_0 = -231.671$ K.

dynamic behavior of the system. We have shown the free energy per particle of the system for $R = 0.48$ nm in Fig. 4. As we know, the free energy function logarithmically diverges as the density approaches to zero which is approved by our results.

One of the important aspects of free energy is finding the equation of state by the following relation,

$$P(\mathfrak{n}, T) = \frac{\mathfrak{n}^2}{\pi R^2}(\frac{\partial f}{\partial \mathfrak{n}})_T, \tag{21}$$

where $\mathfrak{n}$ is number density ($\mathfrak{n} = \frac{N}{L}$). The equation of state has been plotted in Fig. 5 for $R = 0.48$ nm at different temperatures. By reduction of temperature, the pressure curves approach to a characteristic temperature where slope is zero. Now if we divide this curve into two regions (left and right of characteristic temperature), in both the pressure increases by rising the density but this enhancement is different. At left, it is slow whereas at right it is extremely fast. They belong to a gas and liquid states respectively which demonstrate a liquid-gas second order phase transition. Therefore we can call the characteristic temperature as critical temperature (T_c). If we proceed with reduction of the temperature, the curves will possess minimum and maximum points (about $T = 1$ K). Between these extremum points the equation of state curve has a negative slope which can be justified by Maxwell construction. By the aid of these extremum points, we are able to draw phase-diagram of the system which have been presented in Fig. 6. At the bottom of the phase transition curve the system is located in a gas state, but by increasing the density, the bound state of ^{3}He atoms start to construct helium droplets. Finally above the curve, the system completely is in a liquid state. Here we have obtained the critical temperatures and their corresponding

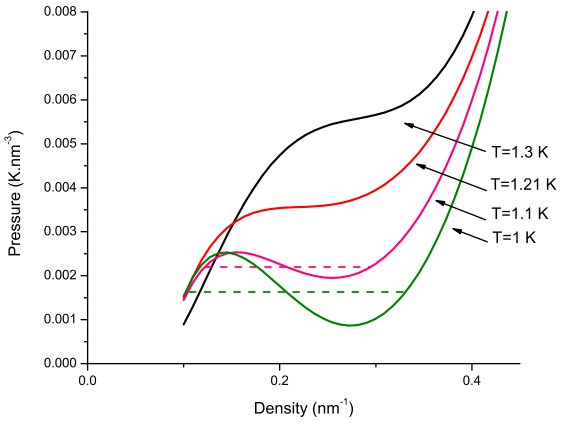

Fig. 5 – Pressure *versus* density (equation of state) for radius ($R = 0.48$ nm) at different temperatures (T).

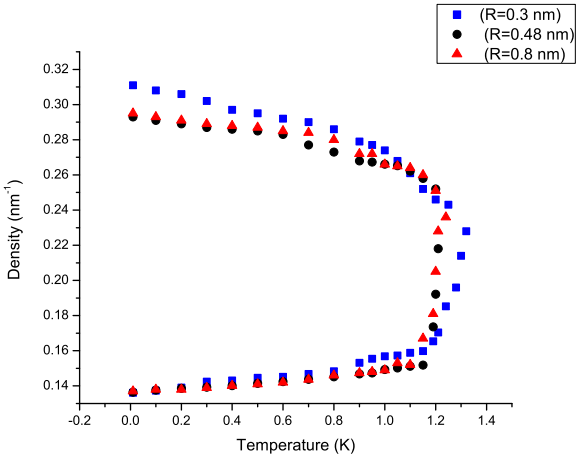

Fig. 6 – Liquid-gas phase diagram for three radii (R).

Table 1

Critical temperature (T_c), critical density ($\mathfrak{n}_c$) and critical pressure (P_c) for fluid ^{3}He confined in a SWCN for three different radii ($R_1 = 0.3,\ R_2 = 0.48,\ R_3 = 0.8$ nm). The results for the bulk case of this system are given for comparison [39].

	R_1	R_2	R_3	Bulk
T_c (K)	1.32	1.21	1.24	3.317
$\mathfrak{n}_c$ (nm^{-1})	0.228	0.218	0.236	8.27
P_c (K·nm^{-3})	0.231	0.227	0.238	8.46

densities which have been presented in Table 1 for different radii. By paying attention to the table shown above, we recognize that by increasing the radius of carbon nanotube, $\mathfrak{n}_c$ do not obey a monotonic behavior. In fact by increasing the radius of carbon nanotube from $R = 0.3$ nm to $R = 0.48$ nm, $\mathfrak{n}_c$ decreases but after $R = 0.48$ nm it increases until it reaches the bulk values. The reason is that in $R = 0.48$ nm, almost all of ^{3}He particles are found in the minimum point of Stan-Cole potential and they experience a unified state, thus, the liquefaction occurs in lower densities. The corresponding results for the bulk case have been also demonstrated for comparison in Table 1. As it is clear, confinement has an strong effect on the critical properties.

The next step is the verification of some response functions of the system such as isothermal compressibility (K_T) and specific heat (C_v). The compressibility has been computed for $T = T_c$ which has been depicted in Fig. 7. As we see all of the curves diverge at critical points, and the limiting behavior is also compatible with the common thermodynamic rules. As the density approaches to zero, the compressibility increases whereas by increasing the density (after liquefaction), it will be almost impossible to compress the fluid. We have shown the specific heat for $\mathfrak{n} = 0.2$ and 1.0 nm^{-1} in Figs. 8 and 9.

In Fig. 8, we see that since $\mathfrak{n} = 0.2$ nm^{-1} is very close to $\mathfrak{n}_c$ the divergence behavior has been appeared. In both Figs. 8 and 9, the specific heat obey the limiting conditions. As the temperature approaches zero, the specific heat approaches zero too, and at high enough temperatures, the specific heat approaches to $\frac{1}{2}$. This result confirms that not only our system experiences a Q1D environment, but also by increasing the temperature, the inter-atomic interaction will be trivial, and also the system behaves like a classical one-dimensional gas. It should be noted that $C_v = \frac{1}{2}$ is related to a 1D non interacting fluid at classical limit. Here we also see that the divergence of compressibility is more extreme than the specific heat. In the next section we will see that this behavior leads to a higher value critical exponent related to the compressibility compared to the specific heat for this quasi-one dimensional fluid. If we compare the critical pressure and temperature of the liquefaction of ^{3}He atoms in SWCN with the bulk case [39], we recognize that by a SWCN environment,

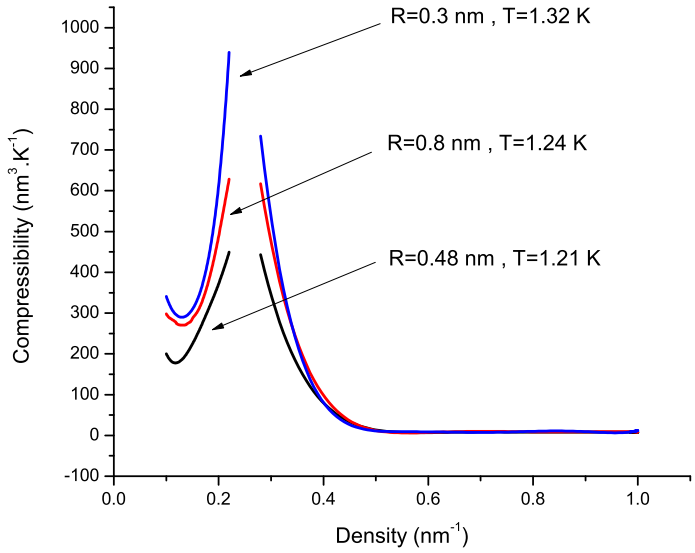

Fig. 7 – Compressibility *versus* density for three radii (R) at their corresponding critical temperatures

we can liquefy ^{3}He atoms in 10^{-1} times lower pressure. Since as it is known, the liquefaction of ^{3}He is an exhausting and costly process. It should be noted that quasi-one dimensional liquid ^{3}He with no confinement does not show any phase transition between $T = 1 \div 4$ K [6], therefore we can conclude that this induced liquefaction is the result of interacting with the carbon atoms of nanotube. In statistical mechanics, there exist some critical exponents that show the divergence behavior of a system close to the critical conditions with respect to different parameters. In the next section, we investigate these critical exponents for our confined system.

4. CRITICAL BEHAVIOR OF FLUID ^{3}He CONFINED IN A SWCN

The order parameter $|n_{liquid} - n_{gas}|$ which is defined to investigate the critical behavior of a system, vanishes at the critical point. However, other thermodynamic properties diverge at this point. Here, the critical exponents are defined to study the asymptotic behavior of singular thermodynamic functions near the critical point. For this purpose, the following functions for the thermodynamic quantities are introduced [37].

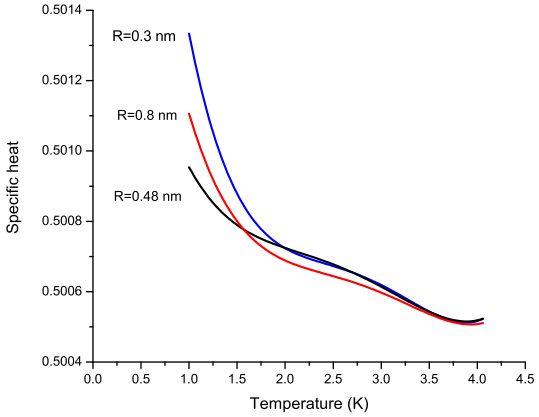

Fig. 8 – Specific heat *versus* temperature for three radii (R) at $\mathfrak{n} = 0.2$ nm^{-1}

4.1. ORDER PARAMETER

We can define the exponent β for the order parameter as follows,

$$|n_l - n_g| \sim (t)^{\beta} \;\; ; \;\; t \to 0^{+}, \tag{22}$$

where,

$$t = \frac{T_c - T}{T_c}. \tag{23}$$

The critical exponent β characterizes the behavior of the order parameter and of course, the earlier function is meaningful only below the critical point in the region where the order parameter is not zero. To obtain β, we draw the order parameter as a function of t on the log-log scale, where the slope will be the value of β.

4.2. PRESSURE

By defining the exponent δ, we can describe the critical isotherm pressure at critical temperature (P_c),

$$|P - P_c| \sim |\mathfrak{n} - \mathfrak{n}_c|^{\delta} \;\; ; \;\; \mathfrak{n} \to \mathfrak{n}_c. \tag{24}$$

We can compute δ by calculating the slope of $\log|P - P_c|$ as a function of $\log|\mathfrak{n} - \mathfrak{n}_c|$.

4.3. SPECIFIC HEAT

The exponent α and α' characterize the behavior of specific heat (C_v) below and above the critical temperature, respectively. For the critical isochore process we

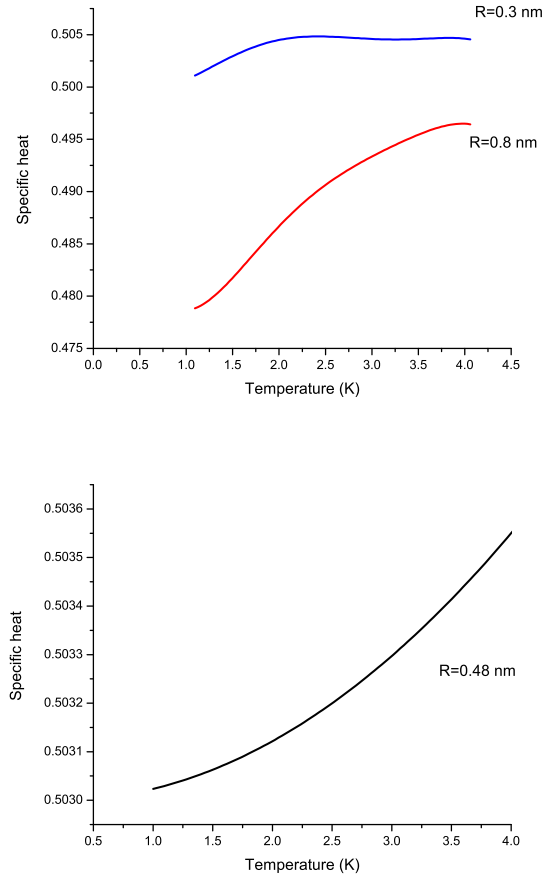

Fig. 9 – Specific heat *versus* temperature for three radii (R) at $\mathfrak{n} = 1.0$ nm^{-1}

would have,

$$C_v = \begin{cases} (-t)^{-\alpha} & ; \ t \to 0^- \\ (t)^{-\alpha'} & ; \ t \to 0^+. \end{cases} \tag{25}$$

4.4. ISOTHERMAL COMPRESSIBILITY

For describing the behavior of isothermal compressibility (K_T) near the critical point, the exponents γ and γ' are defined to be,

$$K_T = \begin{cases} (-t)^{-\gamma} & ; \ t \to 0^- \\ (t)^{-\gamma'} & ; \ t \to 0^+. \end{cases} \tag{26}$$

We have reported the whole critical exponents in Table 2. The corresponding data for

Table 2

As Table 1, but for the critical exponents.

Critical exponent	R_1	R_2	R_3	Bulk
β	0.523	0.681	0.621	0.361
δ	2.163	2.412	2.668	4.21
α	0.343	0.353	0.342	0.105
α'	0.342	0.344	0.338	0.105
γ	0.602	0.272	0.394	1.17
γ'	0.601	0.271	0.392	1.17

the bulk case of fluid ^{3}He have been also given for comparison. As we see there is a substantial difference between the results of quasi-one dimensional for the critical exponents and the results of bulk case. This indicates that the confined fluid ^{3}He has a different thermodynamic behavior near the critical point with respect to that in the bulk case. We have also checked our results for the critical exponents by Griffiths inequality [38],

$$\alpha+\beta(1+\delta)\geq 2. \tag{27}$$

Here, we have found that although the critical exponents of this low dimensional system are different compared to those of the bulk case, they satisfy the above inequalities. Statistical mechanics states that if a system places in a critical temperature or density, its corresponding critical exponents should obey the following relation without attention to what are the particles of the system or what is the interacting potential,

$$\alpha+2\beta+\gamma=2, \tag{28}$$

called, scaling hypothesis [40]. This relation shows a universality for critical systems. The satisfaction of this relation with our results is notable.

5. SUMMARY AND CONCLUSION

In this paper, we have used a variational approach based on the quantum cluster expansion of energy to study the thermodynamic behavior of fluid ^{3}He injected in a single wall carbon nanotube at finite temperature ($T=1\div 4$ K). We have used the Lennard-Jones potential (V_{LJ}) for ^{3}He-^{3}He interaction, and the Stan-Cole potential (V_{SC}) for ^{3}He-C interaction. Our calculations have been done for density range $0.1-1.0$ nm^{-1} and radii $R=0.3$, 0.48 and 0.8 nm. At first, we have calculated the total energy and entropy to obtain the free energy of the system. Our results for the equation of state of quasi-one dimensional fluid ^{3}He show a liquid-gas second order phase transition. Transition points occur in ($T_c=1.32$, 1.21 and 1.24

K) with densities ($\mathfrak{n}_c = 0.228$, 0.218 and 0.236 nm^{-1}) for radii $R = 0.3$, 0.48 and 0.8 nm, respectively. We have plotted the phase-diagram of the system for the mentioned range of densities by determination of the maximum and minimum points of isothermal $P - \mathfrak{n}$ diagram. To verify the transition points more accurately, we have calculated some response functions such as compressibility and specific heat. They demonstrate a second order phase transition in critical points too. The relevant critical exponents have been calculated and checked by Griffiths inequality. The most remarkable achievement of this study is that the liquefaction of ^{3}He in SWCN requires 10^{-1} times lower pressure than unconfined helium. This induced liquefaction related to strong adsorption of ^{3}He particles by carbon atoms. It is found that the critical characteristics of confined quasi-one dimensional fluid ^{3}He are substantially different from those of the bulk case of this system. Another point that should be noted is the concept of phase transition for the one dimensional (1D) and quasi-one dimensional (Q1D) systems. Although phase transition is prohibited for the exactly one dimensional systems, it is admissible in quasi-one dimension. This shows that thermodynamic behavior of quasi-one dimensional systems have extensive differences with the exactly 1D or 2D systems. As a further study, we are interested in verifying the thermodynamic properties of two-dimensional fluid ^{3}He confined by a strongly interacting substrate like graphene.

Acknowledgements. We wish to thank Shiraz University Research Council for financial support. G. H. Bordbar also wishes to thank Physics Department of University of Waterloo for the great hospitality during his visiting. G. H. Bordbar also wishes to thank Prof. Michel Gingras for his guides during this work.

REFERENCES

1. B. D. Marco and D. S. Jin, Sci. **285**, 1703 (1999).
2. S. Jochim, M. Bartenstein, A. Altmeyer, G. Hendl, S. Riedl, C. Chin, J. H. Denschlag, and R. Grimm, Sci. **302**, 2101 (2003).
3. S. Nascimbène, N. Navon, S. Pilati, F. Chevy, S. Giorgini, A. Georges, and C. Salomon, Phys. Rev. Lett. **106** 215303 (2011).
4. M. Greiner, O. Mandel, T. Esslinger, T. W. Ha Ènsch, and I. Bloch, Nature **415**, 39 (2002).
5. R. Combescot and X. Leyronas, Phys. Rev. A. **78** 053621 (2008).
6. H. Kim and D. A. Huse, Phys. Rev. A. **86** 053607 (2012).
7. F. Chevy and C. Mora, Rep. Prog. Phys. **73** 112401 (2010).
8. L. Vranjes, S. Kilic, and E. Krotscheck, J. Low Temp. Phys. **134**, 73 (2004).
9. Y. Okaue and D. S. Hirashima, J. Phys. Chem. Solids. **66**, 1524 (2005).
10. L. Vranje, Z. Antunovi, and S. Kilic, Physica **B 329**, 276 (2003).
11. L. Vranje, Z. Antunovi, and S. Kilic, Physica **B 349**, 408 (2004).
12. G. H. Bordbar, M. A. Rastkhadiv, Phys. Chem. Res. **2**, 252 (2014).
13. Y. Okaue, Y. Saiga, and D. S. Hirashima, J. Phys. Jpn. **75**,053603 (2006).
14. D. Sato, K. Naruse, T. Matsui, and H. Fukuyama, Phys. Rev. Lett. **109**, 235306 (2012).

15. M. M. Calbi, M. W. Cole S. M. Gatica, M. J. Bojan, and G. Stan, Rev. Mod. Phys. **73**, 857 (2001).
16. M. C. Gordillo and J. Boronat, Phys. Rev. Lett. **116**,145301 (2016).
17. G. H. Bordbar and M. A. Rastkhadiv, Mod. Phys, Lett. B. **31**, 1750228 (2017).
18. S. M. Gatica, E. S. Hernañdez, and L. Szybisz, Phys. Rev. **B68**, 144501 (2003).
19. N. Hamada, S. Sawada, and A. Oshiyama, Phys. Rev. Lett. **68**, 1579 (1992).
20. G. H. Bordbar, S. M. Zebarjad, and F. Shojaei, Int. J. Theor. Phys. **43**, 1863 (2004).
21. G. H. Bordbar, S. M. Zebarjad, M. R. Vahdani, and M. Bigdeli, Int. J. Mod. Phys. **B19**, 3379 (2005).
22. G. H. Bordbar, M. J. Karimi, and J. Vahedi, Int. J. Mod. Phys. **B23**, 113 (2009).
23. G. H Bordbar and M. Karimi, Int. J. Mod. Phys. **B23**, 2373 (2009).
24. G. H Bordbar, M. Karimi, and A. Poostforush, Eur. Phys. J. **B73**, 85 (2010).
25. G. H Bordbar and M. Karimi, Int. J. Mod. Phys. **B25** 4359 (2011).
26. G. H Bordbar, S. Mohsenipour, and M. Karimi, Int. J. Mod. Phys. **B25**, 2355 (2011).
27. G. H Bordbar and S. Hoseini, Iranian J. Sci. Tech. **A36**, 225 (2012).
28. G. H Bordbar and N. Mashayekhizade, Phys. Chem. Res. **2**, 90 (2014).
29. G. H. Bordbar, F. Fatemi, and M. T. Mohammadi Sabet, J. Theor. Comput. Chem. **12**, 1350061 (2013).
30. G. H. Bordbar, R. Feridoonnezhad, and M. Taghizade, Rom. J. Phys. **60**, 1010 (2015).
31. G. H. Bordbar and Z. Rezaei, Rom. J. Phys. **61**, 413 (2016).
32. G. H. Bordbar and M. Modarres, Phys. Rev. **C57**, 714 (1998).
33. J. de Boer and A. Michels, Physica **6**, 409 (1939).
34. G. Stan and M. W. Cole, Surf. Sci. **395** 280 (1998).
35. J. W. Clark, Prog. Part. Nucl. Phys. **2** 89 (1979).
36. G. H. Bordbar and M. Modarres, J. Phys. G: Nucl. Part. Phys. **23**, 1631 (1997).
37. C. Garrod, Statistical Mechanics and Thermodynamics, Oxford University Press (1995).
38. R. B. Griffiths, J. Chem. Phys. **43**, 1958 (1965).
39. C. Pittman, T. Doiron, and H. Meyer, Phys. Rev B **20** (1979).
40. R. K. Pathria, "Statistical Mechanics " (Hartnolls Limited Bodmin, Cornwall, 1996).